Marine Geology 369 (2015) 153–161

Contents lists available at ScienceDirect

Marine Geology

journal homepage: www.elsevier.com/locate/margeo

The role of cohesion and overconsolidation in submarine slope failure

Matt J. Ikari *, Achim J. Kopf

MARUM, Center for Marine Environmental Sciences, University of Bremen, Germany

ARTICLE INFO

Article history:
Received 23 April 2015
Received in revised form 10 August 2015
Accepted 18 August 2015
Available online 22 August 2015

Keywords:
Submarine landslide
Slope stability
Overconsolidation
Cohesion
Shear strength
Friction

ABSTRACT

Factor-of-safety analyses of submarine slope failure depend critically on the shear strength of the slope material, which is often evaluated with residual strength values and for normally consolidated sediments. Here, we report on direct measurements of both shear strength and cohesion for a quartz–clay mixture over a wide range of overconsolidation ratios (OCRs). For normally consolidated sediment at low stresses, cohesion is the dominant source of shear strength compared to friction. Significant increases in peak shear strength occur for OCR > 4, and the primary source of this strength increase is due to increased cohesion, rather than friction. The proportion of added shear strength due to cohesion depends log-linearly on the OCR. We show that at shallow depths where OCR values can be high, overconsolidated clays can be stronger than pure or nearly pure quartz sediments, which are cohesionless under near-surface conditions. Our data also suggest that areas which have experienced significant unroofing due to previous mass movements are less likely to experience subsequent failure at shallow depths due to increased peak strength, and if failure occurs it is expected to be deeper where the OCR is lower. In seismically active areas, this is one potential explanation for the general observation of lower slope failure recurrence compared to rates expected from triggering due to local earthquakes.

1. Introduction

The shear strength of sediment and rock is a fundamental property that is a primary control on deformation and structure of the crust. One specific example is in shallow sediments, where the shear strength controls the occurrence of both subaerial and submarine landslides and other types of mass movement (e.g. Hampton et al., 1996; Locat and Lee, 2002; Lee et al., 2007). A popular and simple method of slope failure analysis is the infinite slope factor-of-safety analysis, in which failure of a potential plane parallel to the seafloor (or earth surface in subaerial cases) depends on whether the shear stress on the plane exceeds the shear strength of the material (Morgenstern, 1967; Hampton et al., 1996; Sawyer et al., 2012). Modifications can be made to include effects of earthquakes and excess pore fluid pressure (e.g. Lee and Edwards, 1986; ten Brink et al., 2009; Stigall and Dugan, 2010; Ikari et al., 2011).

Factor-of-safety models may be informed by shear strength measurements taken from laboratory friction experiments. It is convenient to express shear strength τ as a function of effective normal stress $\sigma_n{}'$ (applied normal stress minus pore fluid pressure), with the Coulomb–Mohr failure criterion:

$$\tau = \mu\sigma_n{}' + c \quad (1)$$

where μ is the coefficient of internal friction, and c is the cohesive strength, or cohesion (Handin, 1969; Byerlee; 1978). In this manner, the depth-dependence of shear strength can be estimated. Furthermore, the shear strength can be divided into a frictional portion ($\mu\sigma_n{}'$) and a cohesive portion (c); the latter has been frequently ignored in previous studies involving the geologic strength of materials, but is specifically investigated here. Use of the Coulomb–Mohr criterion is subject to two particular sources of uncertainty at low effective stresses: (1) the relation can be quite non-linear (Schellart, 2000), especially for sediments containing clay minerals (Saffer and Marone, 2003; Ikari et al., 2007), and (2) the cohesion may not be constant, as suggested by Byerlee (1978) and demonstrated by Ikari and Kopf (2011).

In this work we focus on clay-type cohesive strength, a low-stress phenomenon that has been suggested to be associated with bonding of hydrated, charged clay mineral surfaces (Ikari and Kopf, 2011). This type of cohesion should be distinguished from cohesion that may develop in framework minerals at high pressure and temperature due to pressure solution or grain welding (Muhuri et al., 2003; Tenthorey and Cox, 2006). Previous measurements of cohesive strength of a clay–quartz sediment mixture at effective normal stresses of ≤2 MPa have shown that clay-type cohesion depends positively on the effective normal stress, and thus inversely on sediment porosity (Ikari and Kopf, 2011). Both the porosity and consolidation state are known to play a key role in sediment strength and slope failure (Lee and Edwards, 1986), however, the links between cohesion, consolidation state, and slope failure have yet to be addressed. In this work, we extend the work of Ikari and Kopf (2011) in order to: (1) more comprehensively describe

* Corresponding author.
E-mail address: mikari@marum.de (M.J. Ikari).

http://dx.doi.org/10.1016/j.margeo.2015.08.012
0025-3227/

the systematics of friction and cohesion in low-stress sediments, and (2) apply our results to submarine slope failure in nature.

2. Experimental methods

For our experiments we used a commercially obtained, natural clay mineral-rich sediment from northern France (Grüne Tonerde, Argiletz Laboratories) and silt-sized quartz. X-ray diffraction (XRD) shows that the clay sediment is composed of 62% phyllosilicate minerals (primarily illite and mixed layer clays) with other major constituents being quartz and calcite. We mixed the quartz and Grüne Tonerde in a 50–50% mixture by dry weight, and added ~25 wt.% distilled water to form a paste composed of ~31% clay minerals. For comparison, we also conducted experiments using 100% silt-sized quartz saturated with distilled water, and a small number of control experiments using a 50–50% mixture saturated with 3.5% NaCl brine to simulate seawater. Grain size analysis shows that 42% of the Grüne Tonerde is finer than 4 μm and 99.6% finer than 63 μm, classifying it as silty clay. When mixed with the quartz it is on the boundary of clayey silt and sand–silt–clay (Shepard, 1954). For the 50–50% mixture with distilled water, which we used for the majority of these experiments, the plasticity index is 19% and the liquid limit is 31%, classifying it as a low-plasticity clay (Craig, 2004). An oedometer consolidation test in the range 16 to 2000 kPa effective stress shows that the 50–50% mixture has a compression index (void ratio loss per logarithmic increase in effective stress) of 0.19, typical of silts (Mitchell and Soga, 2005).

We conducted shearing experiments at room temperature using a Giesa direct-shear apparatus (Fig. 1A) (see Ikari and Kopf, 2011 and Ikari et al., 2013 for further details). For testing the sample paste is cold-pressed into a sample cell of cylindrical volume (56 mm diameter, 25 mm height), and then loaded to applied normal stresses ranging from 16 kPa to 2 MPa. Porous metal frits allow fluid communication with an open pore fluid reservoir (containing distilled water) and dissipation of excess pore pressure during the initial consolidation phase. All samples were allowed to consolidate overnight so that change in sample height became negligible. At this point we consider the sample to be fully drained so that the applied stress is equal to the effective normal stress acting on the sample. The sample volume is housed within a stack of two steel plates, and relative displacement of the plates enforces planar shear deformation in the sample. Shear stress is corrected for a very small (~2–3 kPa) amount of friction between the two plates. Shear velocity in all cases was 0.5 μm/s.

We measure the shear strength τ of our samples (Eq. (1)), typically at 7–8 mm, after attainment of a steady-state value. Most previous friction studies assume negligible cohesion. Therefore, we define an apparent coefficient of sliding friction $\mu_a = \tau/\sigma_n'$ in order to compare with these studies. However, we are also able to directly measure the cohesion by removing the normal load so that $\sigma_n' = 0$ and $\tau = c$. In this study, most of our cohesion measurements are made on sheared samples, thus we define the sliding cohesion c_s, as measured by removing the normal load after shearing the samples so that $\tau = c_s$. We are thus able to partition the shear strength into a cohesive portion (c_s) and frictional portion ($\mu\sigma_n'$) and calculate the internal coefficient of friction μ (Fig. 1B, Table 1). With increasing sample offset, a greater proportion of the sample becomes supported by the forcing block; however we consider cohesive forces to be effective at the interface of the shearing sample halves. Therefore, values of c_s were corrected for sample offset by calculating the area of two overlapping circles, assuming that any adhesion of the sample to the sample holder is negligible. We also report here the sliding cohesion coefficient $\chi_s = c_s/\sigma_n'$ (Ikari et al., 2013).

We conducted two types of shearing tests under loaded conditions: (1) normally consolidated experiments, in which consolidation and shearing is conducted under the same effective normal stress, and (2) overconsolidated experiments, in which the sample is sheared under a smaller effective normal stress than was applied during consolidation. Several normal consolidation experiments were conducted under a wide range of conditions in order to extend previous results of Ikari and Kopf (2011) and to more robustly characterize friction and cohesion in sediments. Overconsolidated experiments were performed specifically to investigate propensity for failure of submarine slope sediments, which can exhibit a wide range of consolidation states in nature. Sliding cohesion was measured at the end of both types of tests (displacement up to ~9 mm), and we also conducted a subset of measurements under overconsolidated conditions, where shearing was stopped upon attainment of a peak strength (<2 mm displacement) in order to more accurately assess the role of cohesion in these cases (Fig. 1C), (see Table 1 for a full list of experiments).

3. Normal consolidation experiments

3.1. Distribution of frictional and cohesive strengths

For normally consolidated silt quartz and clay–quartz, shear strength gradually increases with displacement to reach a residual value without exhibiting a peak in strength. As effective normal stress increases from 16 kPa to 2 MPa, clay–quartz shear strength values increase from 9 to 985 kPa and c_s increases from 5 to 113 kPa (Fig. 2A). Values of μ_a exhibit a decreasing trend with effective normal stress from 0.58 to 0.50. Sliding cohesion coefficient χ_s decreases from 0.31 to 0.06 with increasing effective normal stress, while internal friction increases from $\mu = 0.24$ to ~0.45 (Fig. 2B). The proportion of

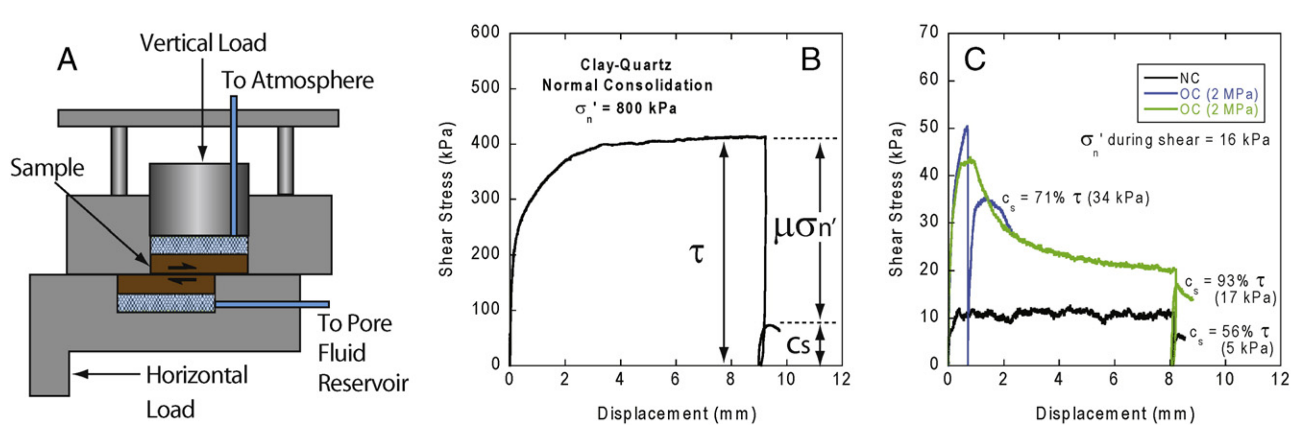

Fig. 1. (A) Schematic illustration of the experimental direct-shear apparatus (not to scale, see text for sample dimensions). (B) Example of a typical shear stress–displacement curve with measurement of shear strength τ and sliding cohesion c_s. The difference is the frictional portion of strength, $\mu\sigma_n'$. (C) Comparison of a normally consolidated (NC) sample with two overconsolidated (OC) samples, one where c_s was measured at the peak strength around 0.7 mm displacement, and one where c_s was measured after 8 mm displacement. Samples were clay–quartz and sheared at 16 MPa, OC samples were consolidated to 2 MPa.